NASA/TM–20210026449

Texas Instruments LM7171 Voltage Feedback Amplifier Laser Single-Event Effects Characterization Test Report

Kaitlyn Ryder

Anthony Phan

Michael Campola

Ani Khachatrian

Dale P. McMorrow

Adrian Ildefonso

January 2022

NASA STI Program Report Series

NASA/TM–20210026449

Texas Instruments LM7171 Voltage Feedback Amplifier Laser Single-Event Effects Characterization Test Report

Kaitlyn L. Ryder
Goddard Space Flight Center, Greenbelt, MD

Anthony M. Phan
Arctic Slope Regional Corporation, Space and Defense AS&D, Inc., Seabrook, MD

Michael J. Campola
Goddard Space Flight Center, Greenbelt, MD

Ani Khachatrian
Naval Research Laboratory, Washington DC

Dale P. McMorrow
Naval Research Laboratory, Washington DC

Adrian Ildefonso
Naval Research Laboratory, Washington DC

Test Date: 7/27/2018
Report Date: 1/5/2022

National Aeronautics and
Space Administration

Goddard Space Flight Center
Greenbelt, MD 20771

January 2022

Acknowledgments

This work was sponsored by the NASA GSFC Radiation Effects and Analysis Group and supported by the On-Orbit Servicing, Assembly and Manufacturing (OSAM-1) mission.

Level of Review: This material has been technically reviewed by technical management.

Available from

NASA STI Program
Mail Stop 148
NASA's Langley Research Center
Hampton, VA 23681-2199

National Technical Information Service
5285 Port Royal Road
Springfield, VA 22161
703-605-6000

This report is available in electronic form at

https://radhome.gsfc.nasa.gov/

1. Introduction

The purpose of this testing was to characterize the pulsed-laser-induced single event effect (SEE) susceptibility of the Texas Instruments LM7171 voltage feedback amplifier. The test was conducted at the U. S. Naval Research Laboratory (NRL) using their pulsed laser setup for SEE testing. Testing occurred on July 27, 2018.

2. Test Samples

The LM7171 is a high speed voltage feedback amplifier that has the slewing characteristic of a current feedback amplifier, yet can be used in all traditional voltage feedback amplifier configurations. The LM7171 is stable for gains as low as +2 or -1. It provides a very high slew rate at 4100 V/µs and a wide unity-gain bandwidth of 200 MHz, while consuming only 6.5 mA of supply current. Operation on the ±15 V power supplies allows for large signal swings and provides greater dynamic range and signal-to-noise ratio. In addition, the LM7171 is specified for ±5 V operation for portable applications.

Five (5) parts from the sample lot of voltage feedback amplifiers were provided for SEE testing. Four (4) of the provided parts were delidded. Two (2) of the delidded parts were nonfunctional during pretesting. DUT1 was used for testing. More information can be found in Table 1.

Table 1: Part Identification Information

Qty	Generic Part Number	LDC	REAG Identifier	Package
5	LM7171BIN/NOPM	N/A	18-016	8-Lead PDIP

3. Test Facility

The laser pulses were generated at NRL by an optical parametric amplifier pumped by a Clark-MXR CPA2110 Ti:Sapphire system. The relevant laser parameters are included below.

Facility:	U. S. Naval Research Laboratory (NRL)
Type of Laser:	Amplified Titanium-Sapphire Laser (Ti:Sapp)
Laser Technique/Setup:	Two-photon absorption; topside irradiation
Wavelength:	1260 nm
Rayleigh Range:	10.6 µm
Beam diameter:	1.34 µm
Pulse Duration:	150 fs
Pulse Repetition Rate:	1 kHz

4. Test Conditions and Error Modes

Test Temperature:	Room temperature
Power Supply Voltages:	±15 V_{DC}
Bias Voltages:	1 V_{DC}
Load Resistances:	2.5 kΩ
Error Modes:	The primary purpose of this test was to identify the worst-case transients. All transients were captured by an oscilloscope.

Below are a series of figures and a table that provide pertinent information related to the set-up. Figure 1 gives the basic schematic of the LM7171. Figure 2 is a circuit diagram of the test board developed for this experiment. Figure 3 is a block diagram of the test set-up. Figures 4 and 5 are pictures of the mounting board constructed for this experiment with the LM7171 test board attached. The perf-board was attached to the optical stage, allowing for a secure connection of the test board to the optical stage. Table 2 contains a list of all the connections in the set-up.

Table 2: Pinout for the LM7171 in the 8-pin PDIP

Pin Number	Description	Connection
1	No Connect	No connection
2	$-V_{IN}$	To common ground
3	$+V_{IN}$	To V_{IN}
4	$-V_S$	To $-V_s$
5	No Connect	No connection
6	OUTPUT	To oscilloscope and load resistors
7	$+V_S$	To $+V_s$
8	No Connect	No connection

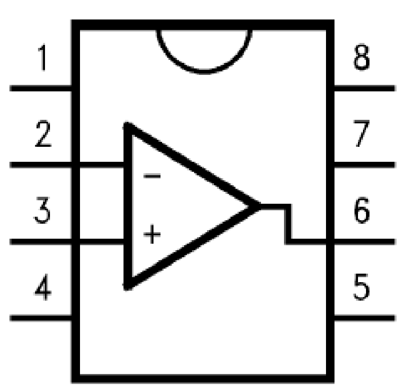

Figure 1. Schematic of the LM7171.

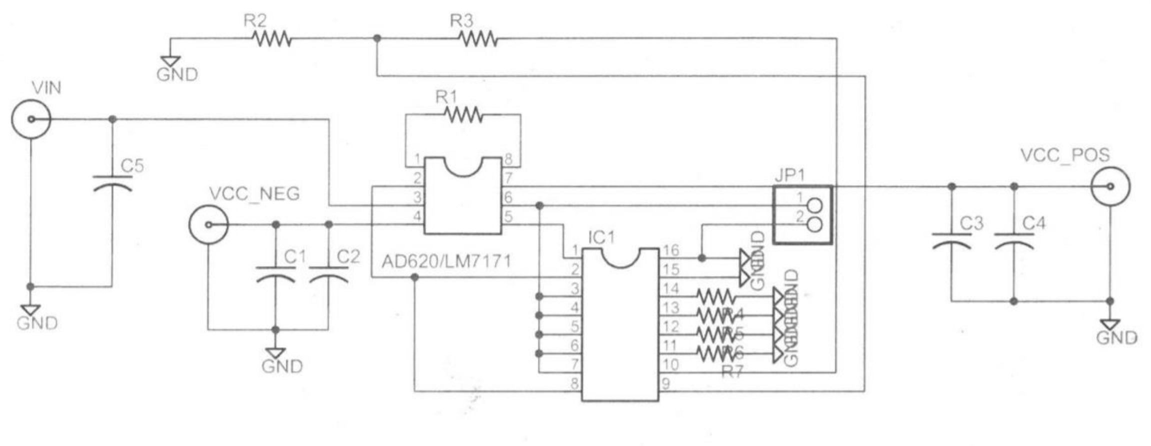

Figure 2. Schematic of the LM7171 test circuit.

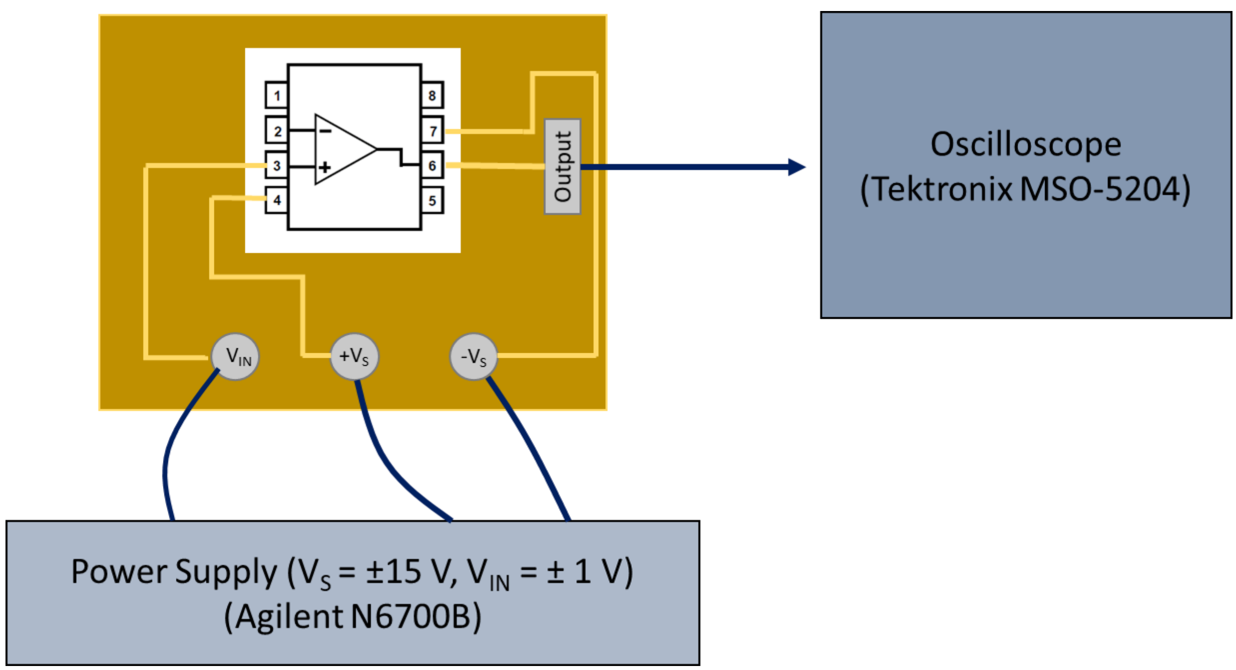

Figure 3. Block diagram of testing set-up.

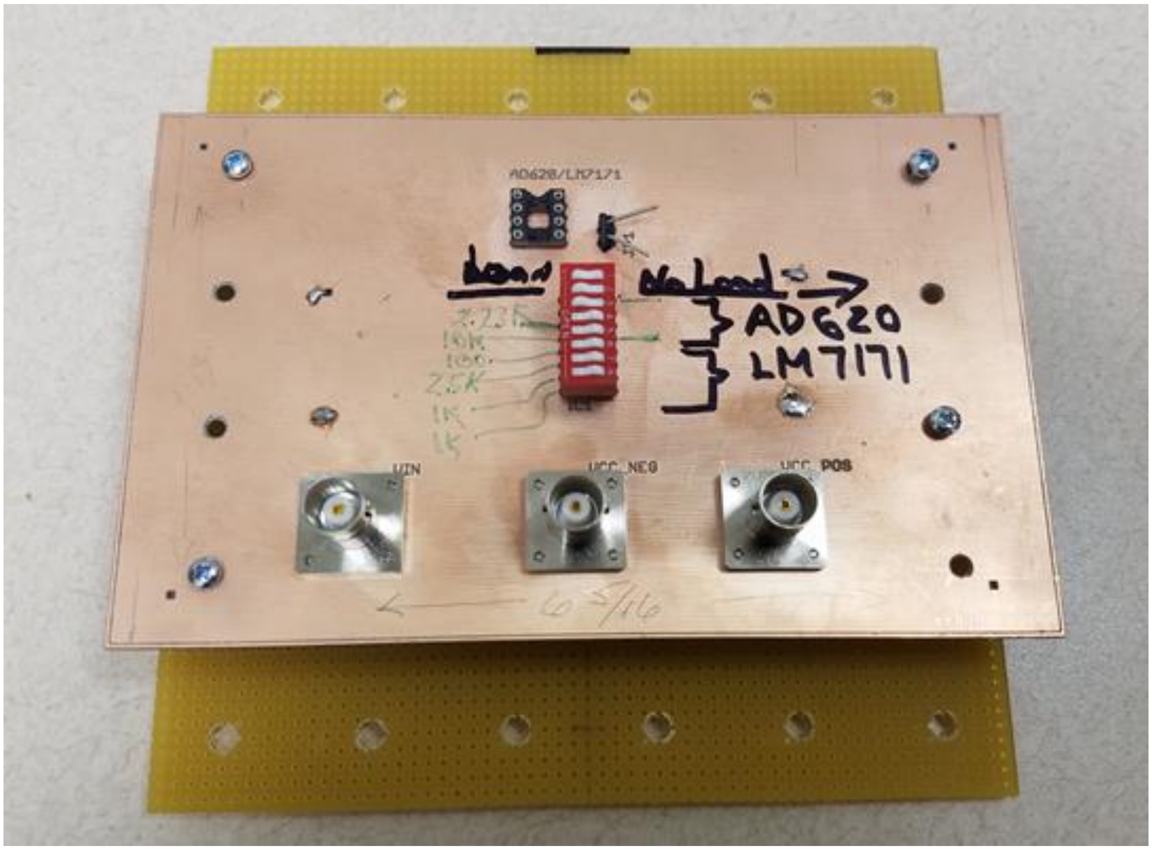

Figure 4. Picture of LM7171 test circuit attached to mounting board.

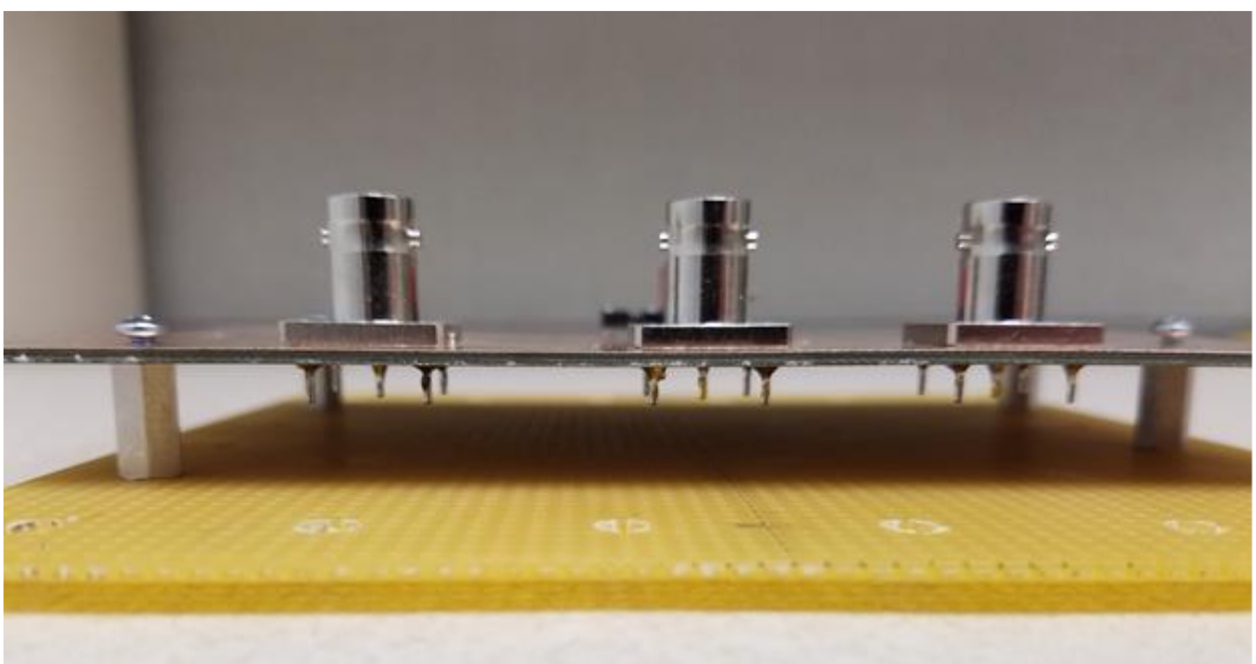

Figure 5. Picture of LM7171 test circuit attached to mounting board.

5. Test Methods

Equipment necessary:

Table 3: List of necessary equipment

Make	Model	NASA ECN	Comments
Tektronix	MSO-5204	2325573	Oscilloscope
Agilent	N6700B	M161838	Power supply
Mounting Board	N/A	N/A	Mounting board
Cables	N/A	N/A	Various cables to make connections

Test Sequence:

Testing was done at various locations on the die as indicated in Figures 6 and 7. For all locations $V_S = \pm 15$ V, $V_{IN} = +1$ V, $R_{Load} = 2.5$ kΩ, and the laser pulse energy ranged from 440 – 540 pJ. The pulse energy was not monitored for individual SETs. A few SETs were captured at each location, sufficient for comparing with results obtained from heavy ion testing. No transients were recorded at location L5. Table 4 lays out the test sequence.

Table 4: Proposed Test Execution Sequence

Run #	Pulse Energy (nJ)	V_S (V)	V_{IN} (V)	R_{Load} (kΩ)	Location (Figures 6, 7)
1	440-540	±15	1	2.5	L1
2	440-540	±15	1	2.5	L2
3	440-540	±15	1	2.5	L3
4	440-540	±15	1	2.5	L4
5	440-540	±15	1	2.5	L5

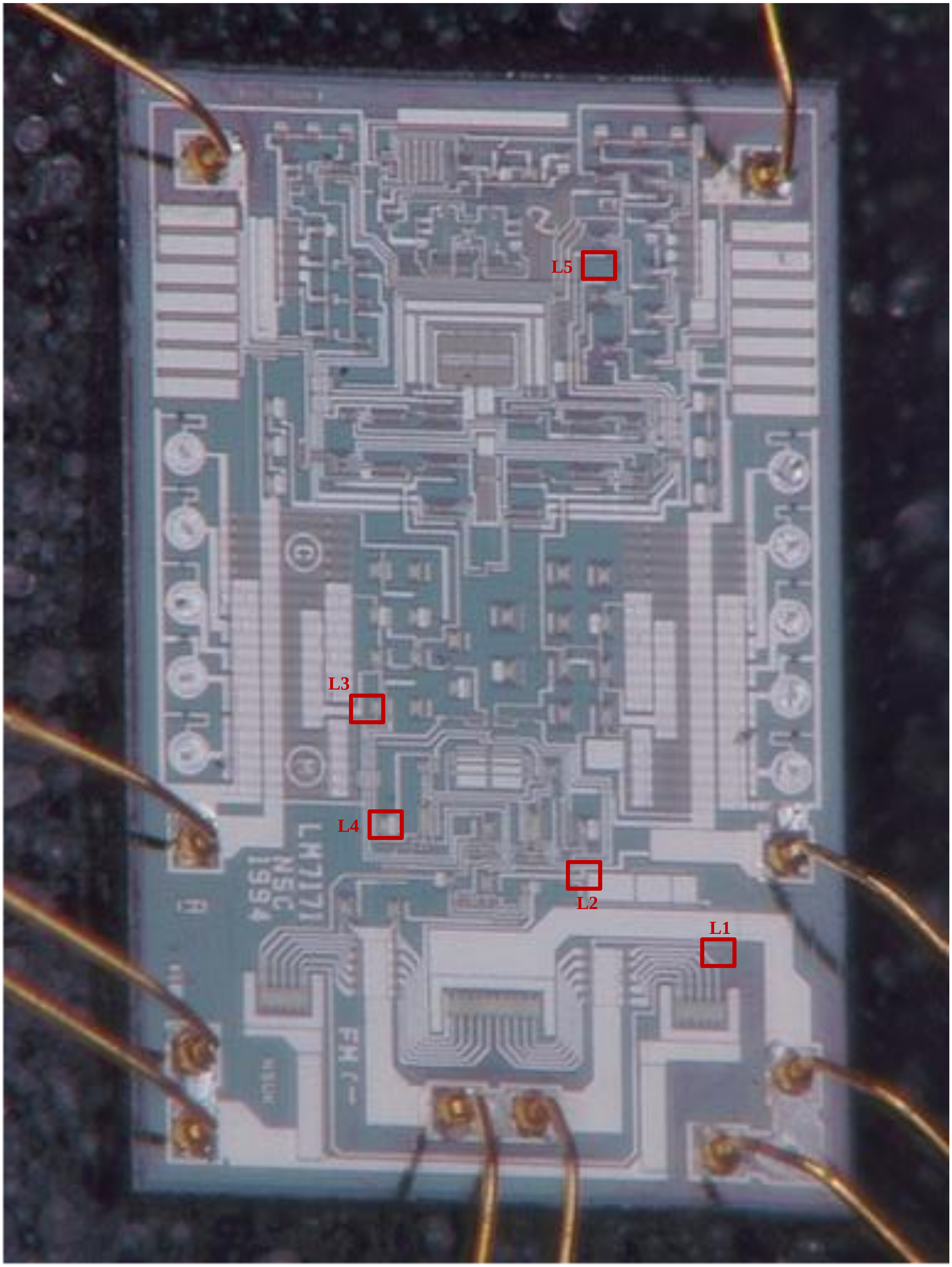

Figure 6. Image of LM7171 die.

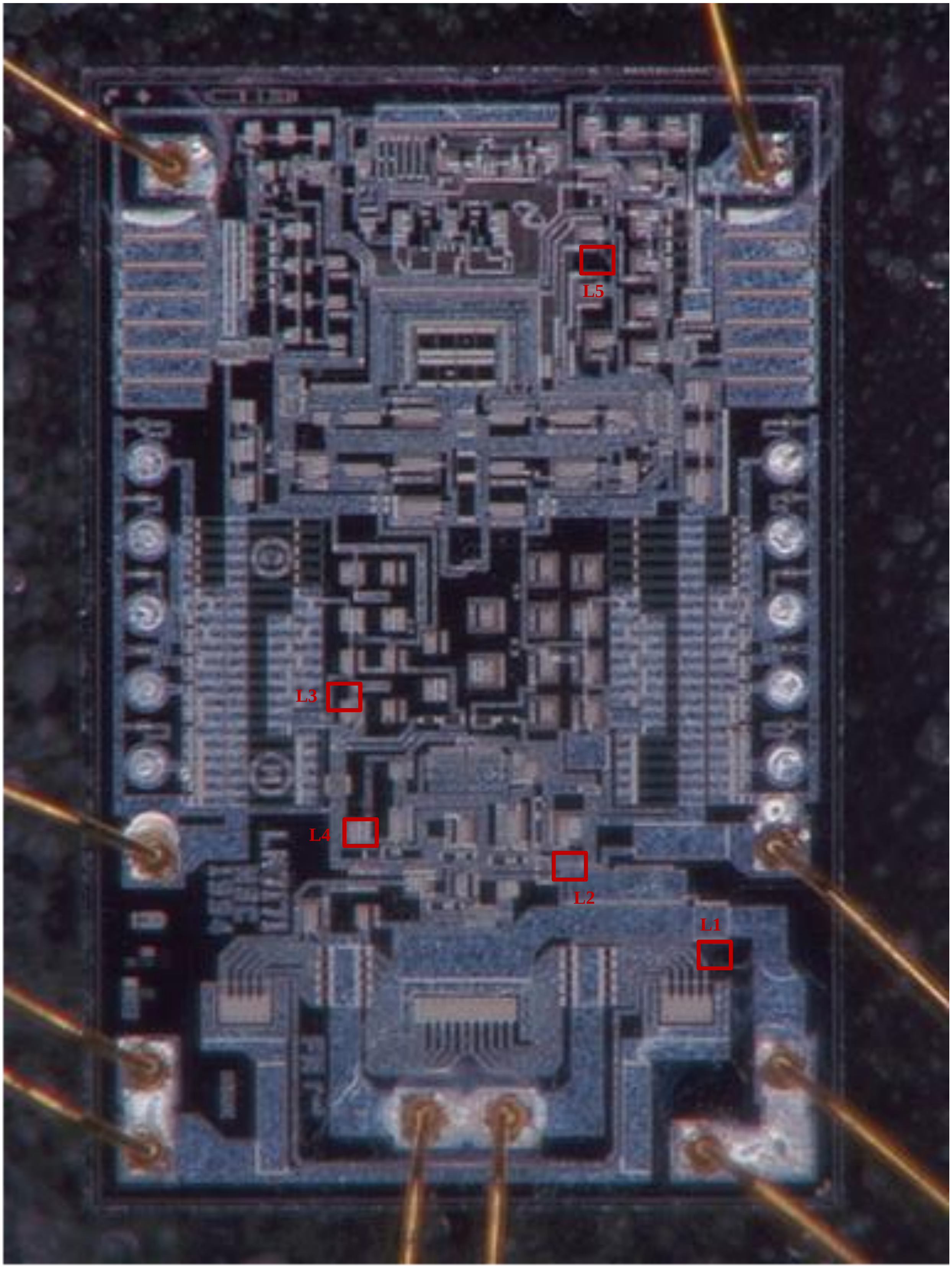

Figure 7. Image of LM7171 die.

6. Test Performance

The test was performed by Kaitlyn Ryder (GSFC-561.0), Michael Campola (GSFC-561.0), Anthony Phan (AS and D Inc.), Ani Khachatrian (NRL) and Adrian Ildefonso (NRL). The test procedure is laid out in general terms in Section 5.

7. Results

One SET was recorded at location L1, shown in Figure 8, which caused a 10 V drop on the output followed by a slow recovery. Other than this one SET, focusing the laser at L1 resulted in noise on the output.

At location L2 the laser focus was moved to different depths in the device, resulting in SETs with different characteristics depending on depth of laser focus. The exact positioning of the laser focus depth was not recorded, so the results are for comparison purposes only. Figures 9 – 11 show three representative SETs that demonstrate show the SETs change with laser focus depth. All SETs show bi-directional characteristics with both positive and negative peaks, but the magnitudes and widths change with laser focus depth. The worst-case SETs at this location show approximately a 2 to 3 V change in voltage over ~100 ns.

At location L3 the laser focus was moved to different depth in the device, resulting in SETs with different characteristics depending on the depth of laser focus. As with location L2, the exact positioning of the laser focus depth was not recorded, and the results are for comparison purposes only. Figures 12 and 13 show two representative SETs observed at L3. All the SETs showed bi-directional characteristics with both positive and negative peaks, but the magnitudes changed with laser focus depth. SETs with large negative-going peaks resulted in the worst-case SETs at this location, with voltage changes of approximately 3 – 4 V over ~100 ns.

The SETs observed at location L4, shown in Figures 14 and 15, were very similar to those from L3. All SETs once again showed bi-directional characteristics, and those with large negative-going peaks had the worst-case magnitudes (3 – 4 V) and durations (~100 ns).

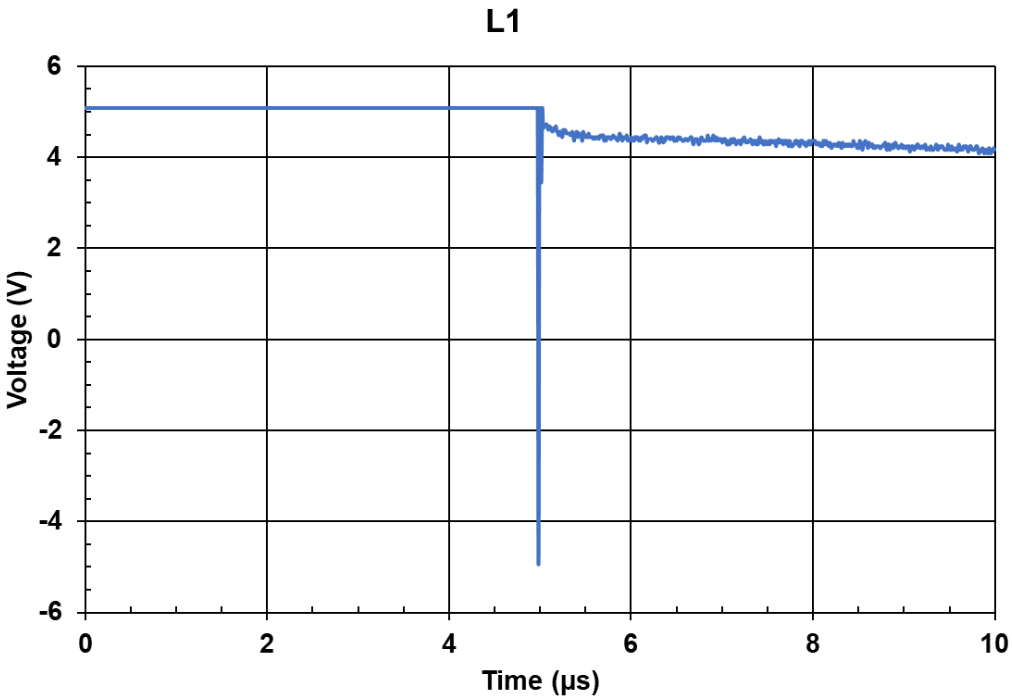

Figure 8. Only recorded SET resulting from the laser being focused at L1.

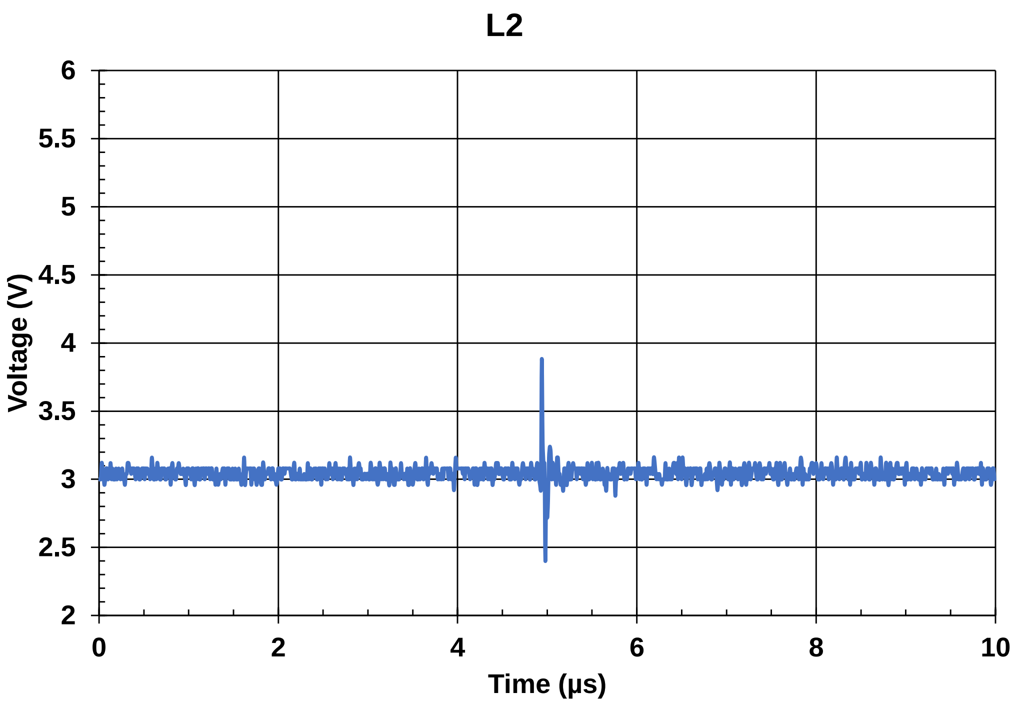

Figure 9. Representative SET with the laser focused at L2.

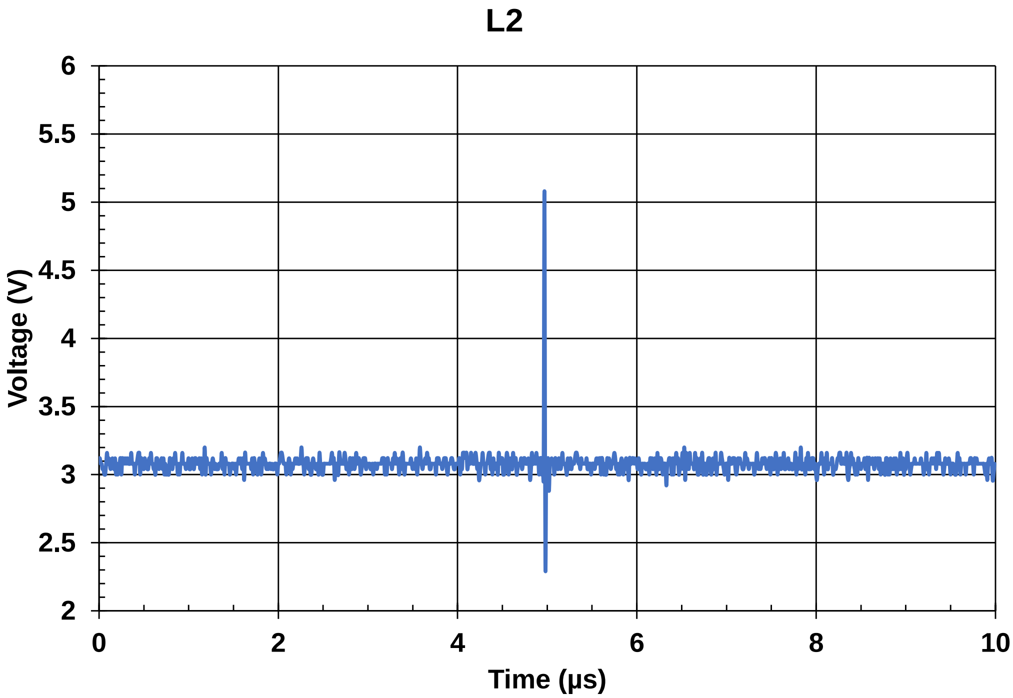

Figure 10. Representative SET with the laser focused at L2.

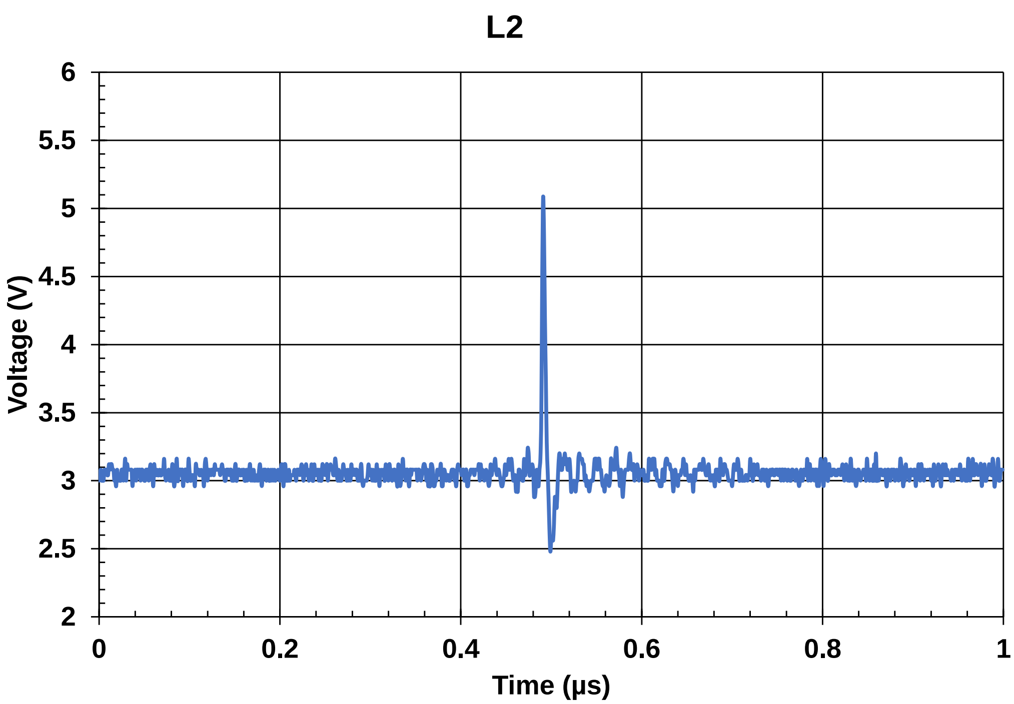

Figure 11. Representative SET with the laser focused at L2. This SET is representative of the worst-case SET observed in terms of magnitude and width.

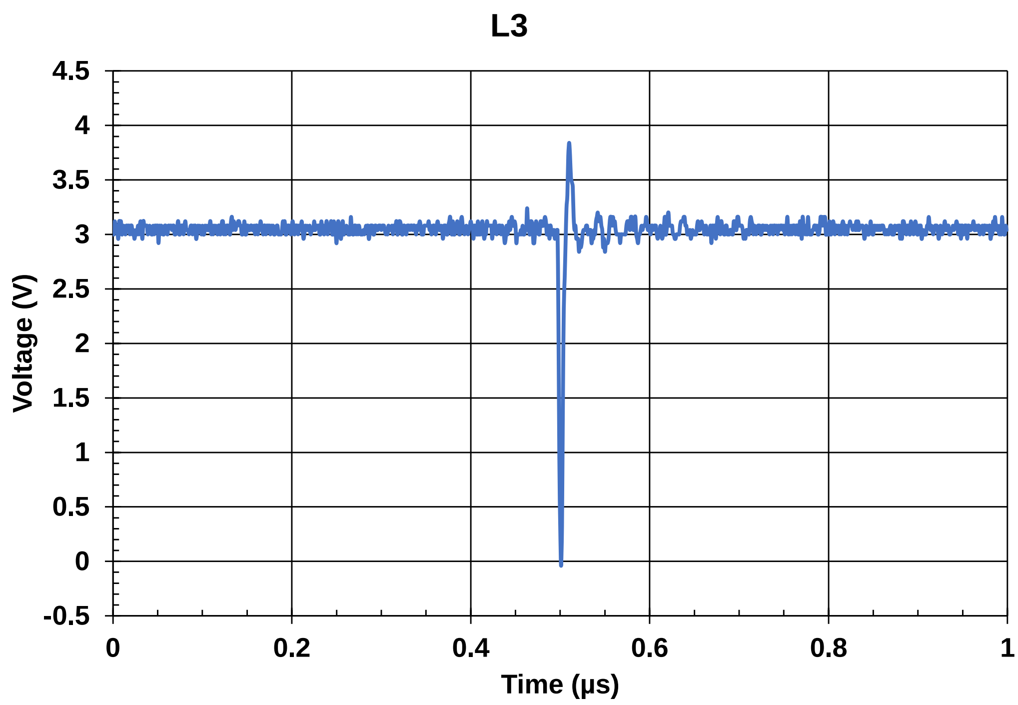

Figure 12. Representative SET with the laser focused at L3. This SET is representative of the worst-case SET observed in terms of magnitude and width.

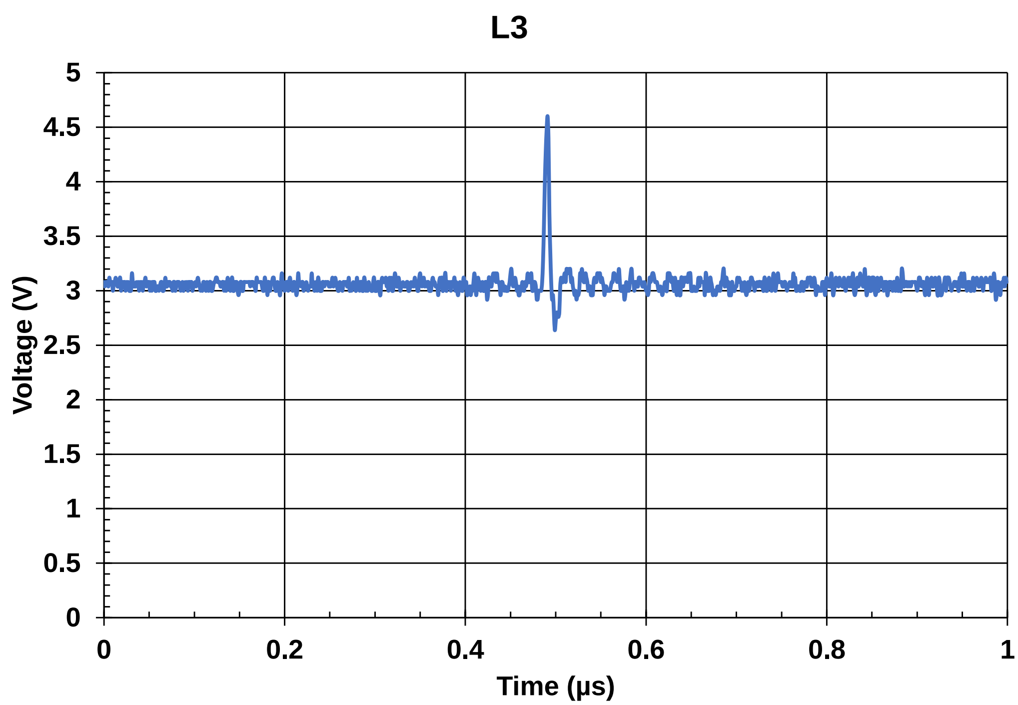

Figure 13. Representative SET with the laser focused at L3.

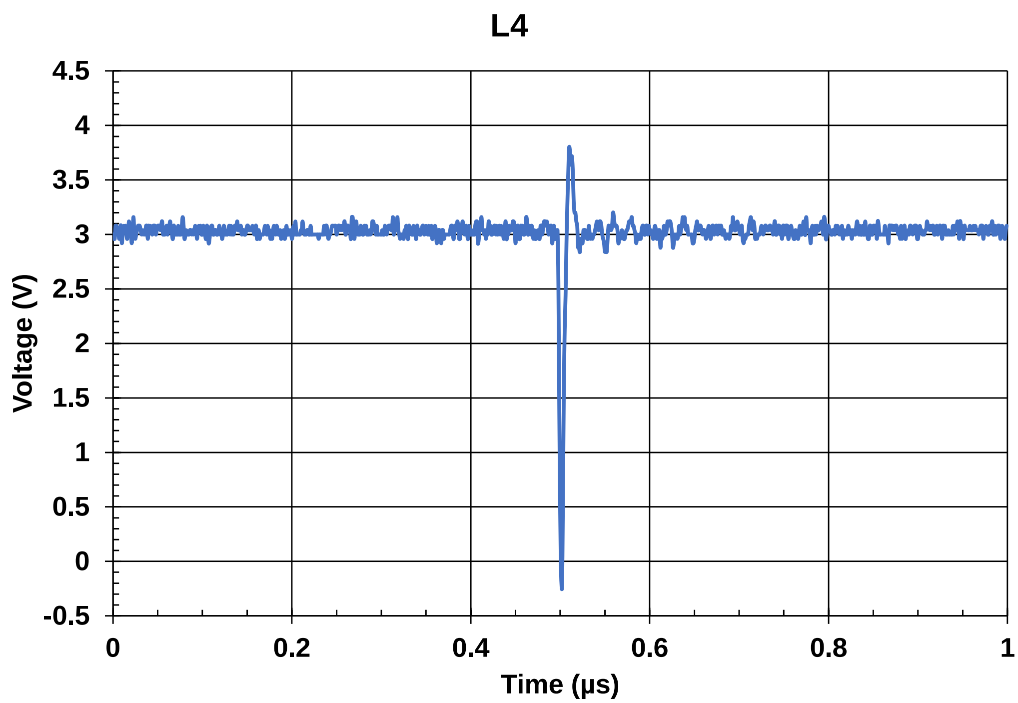

Figure 14. Representative SET with the laser focused at L4. This SET is representative of the worst-case SET observed in terms of magnitude and width.

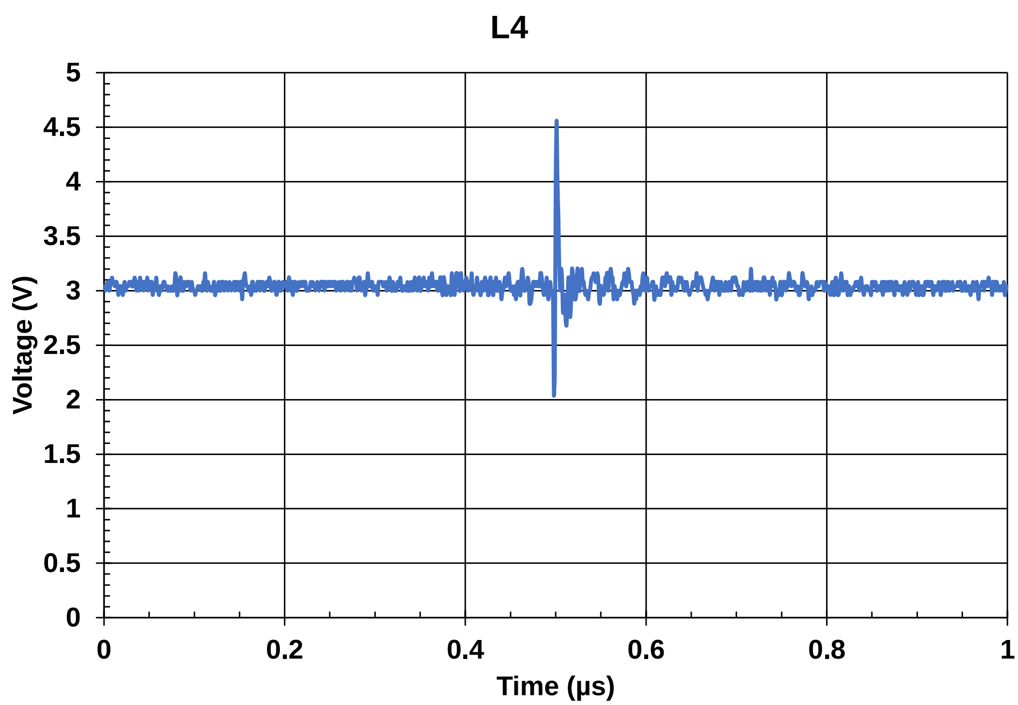

Figure 15. Representative SET with the laser focused at L4.